Ilham Bettahi,[1] Haijing Sun,[1] Nan Gao,[1] Feng Wang,[1] Xiaofan Mi,[1] Weiping Chen,[2] Zuguo Liu,[3] and Fu-Shin X. Yu[1]

Genome-Wide Transcriptional Analysis of Differentially Expressed Genes in Diabetic, Healing Corneal Epithelial Cells: Hyperglycemia-Suppressed TGFβ3 Expression Contributes to the Delay of Epithelial Wound Healing in Diabetic Corneas

Patients with diabetes mellitus (DM) may develop corneal complications and delayed wound healing. The aims of this study are to characterize the molecular signatures and biological pathways leading to delayed epithelial wound healing and to delineate the involvement of TGFβ3 therein. Genome-wide cDNA microarray analysis revealed 1,888 differentially expressed genes in the healing epithelia of normal (NL) versus type 1 DM rat corneas. Gene ontology and enrichment analyses indicated TGFβ signaling as a major altered pathway. Among three TGFβ isoforms, TGF-β1 and β3 were upregulated in response to wounding in NL corneal epithelial cells (CECs), whereas the latter was greatly suppressed by hyperglycemia in rat type 1 and 2 and mouse type 1 DM models. Functional analysis indicated that TGF-β3 contributed to wound healing in NL corneas. Moreover, exogenously added TGF-β3 accelerated epithelial wound closure in type 2 rat and type 1 mouse DM corneas via Smad and PI3K-AKT signaling pathways, autoregulation, and/or upregulation of Serpine1, a well-known TGFβ target gene. Taken together, our study for the first time provides a comprehensive list of genes differentially expressed in the healing CECs of NL versus diabetic corneas and suggests the therapeutic potential of TGF-β3 for treating corneal and skin wounds in diabetic patients.

Diabetes 2014;63:715–727 | DOI: 10.2337/db13-1260

[1]Departments of Ophthalmology and Anatomy and Cell Biology, Wayne State University School of Medicine, Detroit, MI
[2]Genomic Core Laboratory of National Institute of Diabetes and Digestive and Kidney Diseases, Bethesda, MD
[3]Xiamen Eye Center, Key Laboratory of Ophthalmology and Visual Science of Fujian Province, Xiamen University, Xiamen, Fujian, China

Corresponding author: Fu-Shin X. Yu, fyu@med.wayne.edu.

Received 15 August 2013 and accepted 25 October 2013.

This article contains Supplementary Data online at http://diabetes.diabetesjournals.org/lookup/suppl/doi:10.2337/db13-1260/-/DC1.

I.B., H.S., and N.G. contributed equally to this work.

F.W. is currently affiliated with the Department of Ophthalmology, the First Affiliated Hospital of Anhui Medical University, Hefei, Anhui, People's Republic of China.

With the rapid increase in the prevalence of diabetes mellitus (DM), ocular complications have become a leading cause of blindness around the world. In addition to abnormalities of the retina (retinopathy) and the lens (cataracts), various types of corneal disorders are also relatively common in DM patients (1). Hyperglycemia significantly alters epithelial structure and function, resulting in basal cell degeneration (2), decreased cell proliferation (3,4), superficial punctate keratitis (5), breakdown of barrier function, fragility (6,7), recurrent erosions, and persistent epithelial defects (8), depending on the duration of DM and on the serum concentration of glycated hemoglobin HbA_{1c}. The epithelial abnormalities, termed keratopathy/epitheliopathy, are likely the results of these pathological changes and are resistant to conventional treatment regimens (9). Hence, a better understanding of the pathogenesis of diabetic keratopathy should lead to a better management of the disease.

Similar to other mucosal linings, the corneal epithelium is under constant environmental insults, often resulting in tissue injury. Prompt healing of the injured epithelium is vital to maintaining a clear, healthy cornea and for preserving vision (10). Healing involves a number of processes, including cell migration, proliferation, differentiation, apoptosis, and tissue remodeling (11). Hyperglycemia has profound effects on these biological processes. Unlike diabetic retinopathy, diabetic keratopathy does not cause many detectable clinical symptoms unless corneal epithelial cells (CECs) are removed or an eye is injured (12). Delayed epithelial wound healing may lead to sight-threatening complications such as stromal opacification, surface irregularity, and microbial keratitis (9). Hyperglycemia is likely to execute its adverse effects on corneal wound healing by modifying the expression of a host of wound response genes. To date, a genome-wide screen for genes, their associated pathways, and the networks affected by DM in CECs in vivo and their roles in wound closure have not been reported for the cornea.

Recently, we developed/adapted several diabetic models and demonstrated that diabetic rat corneas exhibited a similar pathology of human diabetic keratopathy, including decreased corneal sensitivity, reduced tear secretion, and most important, delayed epithelial wound healing, indicating that these are useful models to study impaired wound healing in diabetic corneas (4,6,7). In this study, we took advantage of an easily procurable epithelial cell population during epithelial debridement and from migrating epithelial sheets that have moved into the original wound bed. Using a genome-wide cDNA microarray, we profiled gene expression in DM and normal (NL) rat CECs. We identified 1,888 probe sets with more than 1.5-fold changes in the healing CECs of DM compared with NL corneas and found transforming growth factor β (TGFβ) signaling as a major pathway affected by hyperglycemia in DM CECs. We further demonstrated for the first time that wound-induced upregulation of TGFβ3 is dampened by hyperglycemia and that exogenously added TGFβ3 accelerated delayed epithelial wound closure in three rodent diabetic models. We proposed that TGF-β3 is a suitable therapeutic for treating delayed diabetic wound healing in peripheral tissues such as the cornea and skin.

RESEARCH DESIGN AND METHODS

Animals and Induction of Diabetes

All investigations conformed to the regulations of the Association for Research in Vision and Ophthalmology Statement for the Use of Animals in Ophthalmic and Vision Research and the National Institutes of Health. Streptozotocin (STZ) induction of type 1 DM Sprague-Dawley (SD) rats was as described (4,7), and type 2 DM Goto-Kakizaki (GK) rats were both maintained in the Kresge Eye Institute animal facility under standard conditions. C57BL/6 (B6) mice were induced to develop type 1 DM according to a low-dose STZ induction protocol (mouse). Glucose levels and body weight were monitored weekly. Animals with blood glucose levels higher than 400 mg/dL (STZ-SD rats), 220 mg/dL (GK rats), and 350 mg/dL (B6 mice) were considered diabetic and were used, with age-matched animals as the control, at 8 weeks after STZ treatment for SD rats, 6 months old for GK rats, and 10 weeks after STZ for B6 mice. These are times when epithelial wound closure is significantly delayed and many pathologies can be observed in the DM animals (6,7,13).

Corneal Epithelial Debridement Wound

Anesthetized rats and mice were first demarcated with a trephine in the central cornea (circular wound of 5 mm for rats and 2 mm for mice), and CECs were removed with a blunt scalpel blade under a dissecting microscope (4,6,7). The blade with scraped CECs was immediately immersed in liquid nitrogen, and the visible ice was collected into a test tube, placed on dry ice, and stored at −80°C. The sample was marked as unwounded (UW). Bacitracin ophthalmic ointment was applied to the cornea after surgery to prevent infection. At 42 h (rats) or 24 h (mice) postwounding (hpw), the same size trephine was used to mark the original wound, and CECs within the circle were removed, collected as described for the original wounding, and marked as healing CECs.

RNA Extraction and Real-Time PCR

For RNA isolation, CECs were scraped off of corneas, with two corneas pooled into one tube as one sample. RNA was extracted from the collected CECs using the RNeasy Mini Kit (QIAGEN). cDNA was generated with an oligo (dT) primer (Invitrogen), followed by analysis using real-time PCR with the Power SYBR Green PCR Master Mix (AB Applied Biosystems), based on the expression of β-actin.

Gene Array and Functional Analysis

cDNAs were synthesized and hybridized to Affymetrix GeneChip Rat Genome 230, and 2.0 array was performed by the Microarray Core Facility at Wayne State University according to the manufacturer's protocols. The

microarray data were evaluated by the Genomic Core Laboratory of the National Institute of Diabetes and Digestive and Kidney Diseases. The ANOVA analysis for the robust multichip average normalized data sets was completed by the commercial Partek Genomic Suite microarray data analysis software (http://www.partek.com/partekgs/). Signaling pathway and functional network analyses were performed using Genomatrix Pathways System software.

Subconjunctival Injection of Small Interfering RNA and Recombinant TGF-β Polypeptides

For mice, 5 μL solution was injected into the subconjunctival space at one site at the superior part of the cornea and for rats, 20 μL at two sites, and 10 μL each at the superior and inferior quadrants. TGF-β3 was injected 4–6 h and short interfering RNA (siRNA) 24 h before wounding.

Immunohistochemistry of Rat, Mouse, and Human Corneas

Rat eyes were enucleated, embedded in Tissue-Tek O.C.T. compound, and frozen in liquid nitrogen. Sections (6 μm thick) were cut and mounted to polylysine-coated glass slides. NL and diseased human corneas obtained from the Midwest Eye Bank were embedded in Tissue-Tek O.C.T. compound immediately upon arrival. The cryostat sections of wounded and healed organ-cultured human corneas of diabetic and age-controlled groups were a gift from Dr. Alexander V. Ljubimov, Cedars-Sinai Medical Center (2). After drying in air, followed by a 10-min fixation in 4% paraformaldehyde, slides were blocked with 2% BSA in PBS for 1 h at room temperature. Sections were then incubated with rabbit primary antibody (TGF-β1, TGF-β2, and TGF-β3 1:50, Abcam). This was followed by fluorescein isothiocyanate anti-rabbit antibody (1:100; Jackson ImmunoResearch Laboratories). Slides were mounted with Vectashield mounting medium containing DAPI and examined under a Carl Zeiss fluorescence microscope Axioplan 2 equipped with an ApoTome digital camera or using confocal microscopy (TCSSP2; Leica). Controls were similarly treated, but the primary antibody was replaced with rat or rabbit IgG.

Determination of Protein Expression and Phosphorylation by Western Blot Analysis

The CECs removed during corneal debridement (the control) and PW, but before wound closure, were collected from NL and diabetic rat corneas and lysed with radioimmunoprecipitation assay buffer. Protein concentrations were determined using a Micro BCA kit. Levels of various proteins or their phosphorylation were determined using specific antibodies. For each condition, two samples were shown with β-actin levels as the internal controls.

Statistical Analysis

Data are presented as means ± SE. Statistical differences among three or more groups were first identified using one-way ANOVA, followed by the Student *t* test for pairwise comparison. Differences were considered statistically significant at $P < 0.05$.

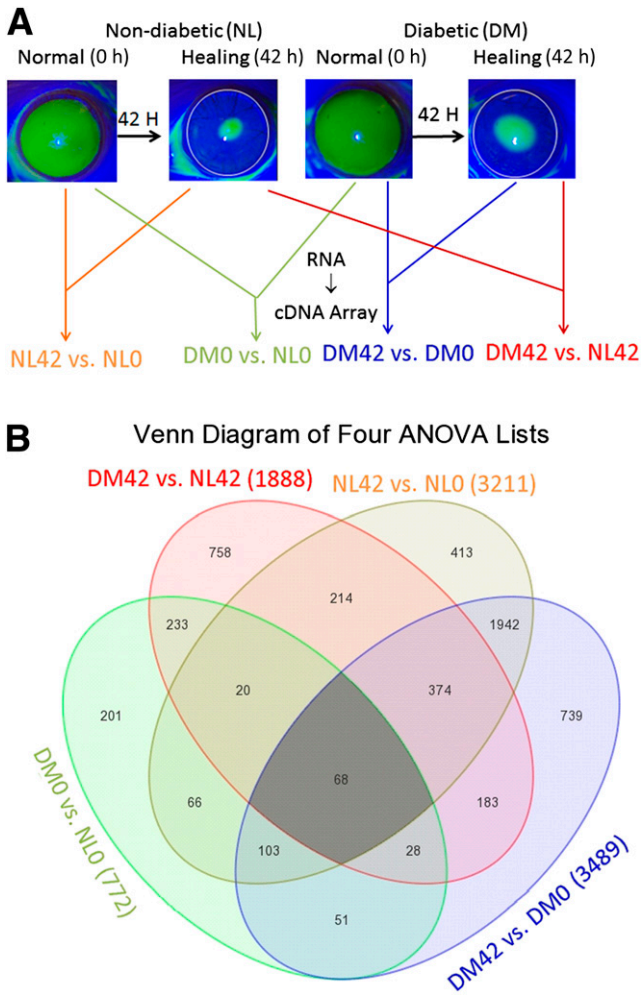

Figure 1—Expression profiling of genes differentially expressed in epithelial cells in response to wounding in STZ diabetic and control, nondiabetic rat corneas. *A*: To create an epithelial debridement wound, the epithelium was marked by a 5-mm trephine, and epithelial cells within the mark were removed and collected as homeostatic CECs. The wounds were allowed to heal for 42 h, and the epithelial cells that migrated into the original wound bed were scraped and referred to as healing CECs. The samples were used for RNA preparation and subjected to Affymetrix GeneChip Rat Genome 230 2.0 Array analysis. Binary comparisons were made as indicated, creating differential expression profiles and significance measures corresponding to the indicated effects, each based on the mean and variance of three independent experiments. *B*: Venn diagrams indicate overlap of genes induced due to wounding in NL and DM rats. The cutoff values are twofold difference for healing vs. homeostatic and 1.5-fold for DM vs. NL. Each circle represents the pairwise comparison indicated.

RESULTS

We previously showed that epithelial wound healing, as seen in DM patients, was significantly delayed in the corneas of STZ-induced type 1 and GK type 2 DM rats compared with the control rats (4,7,13,14). We reasoned

Table 1—Top up- and downregulated genes

Gene symbol	Gene title	Fold change	*P* value
The top 10 most up- and downregulated genes in healing/UW CECs of NL rats			
S100a9*	S100 calcium binding protein A9	705.415	1.64E-10
Serpinb2*	Serine (or cysteine) peptidase inhibitor, clade B, member 2	563.839	2.14E-10
Defb4*	Defensin β 4	372.452	1.03E-09
Car12*	Carbonic anhydrase 12	316.135	1.02E-11
Serpinb10*	Serine/cysteine peptidase inhibitor, clade B, member 10	305.695	2.38E-11
AVLV472	Similar to AVLV472	272.388	1.45E-10
Tnc*	Tenascin C	266.987	5.27E-08
S100a8*	S100 calcium binding protein A8	249.303	9.58E-09
Krt17*	Keratin 17	202.958	2.20E-11
Sprr1b	Small proline-rich protein 1B (cornifin)	202.042	1.23E-06
Tril	TLR4 interactor with leucine-rich repeats	−27.792	7.17E-07
Dync1i1	Dynein cytoplasmic 1 intermediate chain 1	−30.563	4.65E-11
Igfbp5	Insulin-like growth factor binding protein 5	−32.459	5.81E-08
Lrrn3	Leucine rich repeat neuronal 3	−34.154	1.48E-07
Gpm6a	Glycoprotein m6a	−35.599	0.000105
Cps1	Carbamoyl-phosphate synthetase 1	−41.316	9.37E-07
Gad1	Glutamate decarboxylase 1	−41.548	2.44E-08
Tacr2	Tachykinin receptor 2	−42.053	4.29E-07
Cxcl14*	Chemokine (C-X-C motif) ligand 14	−45.971	1.54E-08
Ptpro*	Protein tyrosine phosphatase, receptor type, O	−56.52	1.38E-08
The top 10 most up- and downregulated genes in healing/UW CECs of DM rats			
S100a9*	S100 calcium binding protein A9	458.928	2.81E-10
Serpinb10*	Serine peptidase inhibitor, clade B, member 10	311.583	2.32E-11
Car12*	Carbonic anhydrase 12	273.911	1.25E-11
Defb4*	Defensin β 4	243.856	1.85E-09
Krt17*	Keratin 17	217.086	1.99E-11
Sprr1b	Small proline-rich protein 1B (cornifin)	201.148	1.24E-06
S100a8*	S100 calcium binding protein A8	166.442	1.75E-08
AVLV472	Similar to AVLV472	165.464	3.03E-10
Serpinb2*	Serine (or cysteine) peptidase inhibitor, clade B, member 2	124.377	1.87E-09
Pdpn*	Podoplanin	122.676	6.71E-10
Igfbp5	Insulin-like growth factor binding protein 5	−21.836	1.50E-07
Wnt2*	Wingless-type MMTV integration site family member 2	−21.992	0.000251
Dapl1	Death associated protein-like 1	−23.277	1.34E-06
Gpm6a	Glycoprotein m6a	−24.972	0.000216
Tacr2	Tachykinin receptor 2	−29.366	9.35E-07
Cxcl14*	Chemokine (C-X-C motif) ligand 14	−30.087	3.88E-08
Dync1i1	Dynein cytoplasmic 1 intermediate chain 1	−32.555	4.02E-11
Gad1	Glutamate decarboxylase 1	−34.251	3.71E-08
Cps1	Carbamoyl-phosphate synthetase 1	−46.747	7.29E-07
Ptpro*	Protein tyrosine phosphatase, receptor type, O	−51.929	1.63E-08
The top 10 most up- and downregulated genes in UW DM/NL rat CECs			
Ephx2*	Epoxide hydrolase 2, cytoplasmic	14.8351	4.45E-08
Akr1b8	Aldo-keto reductase family 1, member B8	3.35444	0.033642
Elovl4	Elongation of very long chain fatty acids-like 4	3.18504	0.030089
Ctdspl	CTD (carboxy-terminal domain) small phosphatase-like	2.89265	0.013859
Pdyn*	Prodynorphin	2.88355	0.024604
Col12a1	Collagen, type XII, a 1	2.69369	0.047762
CAMK1D	Similar to calcium/calmodulin-dependent protein kinase 1D	2.66033	0.000102
Lect1	Leukocyte cell derived chemotaxin 1	2.50341	0.000163
Phb2	Prohibitin 2	2.42591	0.014843
Ddah1	Dimethylarginine dimethyl aminohydrolase 1	2.34997	0.004703
Ggt1	γ-Glutamyltransferase 1	−3.1326	0.023773
Mtmr1	Myotubularin related protein 1	−3.3812	0.003785
GBP6	Similar to guanylate binding protein family, member 6	−3.3911	0.002009
Aqp2	Aquaporin 2 (collecting duct)	−3.777	0.025883
Krt8	Keratin 8	−3.7889	0.000127
Wfdc5	WAP four-disulfide core domain 5	−4.4483	0.002422
Gpm6a	Glycoprotein m6a	−4.6711	0.015797
SNX10	Sorting nexin 10	−5.5743	2.27E-05
Fam111a	Family with sequence similarity 111, member A	−8.8546	0.037558
C1ql3*	Complement component 1, q subcomponent-like 3	−10.238	2.65E-06

Continued on p. 719

Table 1 — Continued

Gene symbol	Gene title	Fold change	*P* value
The top 10 most up- and downregulated genes in healing DM/NL rat CECs			
Ephx2*	Epoxide hydrolase 2, cytoplasmic	11.9119	8.65E-08
CD99l2	Similar to MIC2 like 1	3.57749	0.001322
Arid2	AT rich interactive domain 2 (Arid-rfx like)	3.03913	0.007696
Ctdspl	CTD (carboxy-terminal domain) small phosphatase-like	2.66501	0.020035
Gsta4	Glutathione *S*-transferase α 4	2.57045	0.005536
Phgdh	Phosphoglycerate dehydrogenase	2.50389	0.000145
Ahdc1	AT hook, DNA binding motif, containing 1 (*Rattus norvegicus*)	2.46515	0.002914
Phb2	Prohibitin 2	2.37832	0.016485
CD99L2	Similar to MIC2 like 1	2.26117	0.003917
Auts2l	Autism susceptibility candidate 2-like	2.24651	0.007632
Wnt2*	Wingless-type MMTV integration site family member 2	−4.2398	0.019534
Plod2	Procollagen lysine, 2-oxoglutarate 5-dioxygenase 2	−4.2793	2.67E-06
Adm*	Adrenomedullin	−4.5972	0.007971
Fam3b*	Family with sequence similarity 3, member B	−5.1147	0.000102
Postn	Periostin, osteoblast specific factor	−5.4259	0.002689
Ceacam1*	Carcinoembryonic antigen-related cell adhesion molecule 1	−6.4485	0.010465
Cald1	Caldesmon 1	−6.7921	0.002262
Tmem35	Transmembrane protein 35	−7.5325	0.000227
Atf3*	Activating transcription factor 3	−7.5617	0.006267
Vim*	Vimentin	−8.6761	0.000222

*The expression pattern of the genes was confirmed at least by real-time PCR in one or more animal DM models.

that genes induced in response to wounding and affected by hyperglycemia are responsible for the delay of epithelial wound closure in the cornea, and we performed a genome-wide microarray expression analysis to compare the gene expression profiles of CECs collected during the creation of epithelial debridement wounds at 0 h and at 42 hpw from the control, NL, and DM rat corneas (Fig. 1*A*). The rats used were 14 weeks old, with 8 weeks of hyperglycemia, the duration sufficient to affect the rate of epithelial wound closure. Using the Rat Genome GeneChip, we detected 5,426 probe sets differentially expressed at least in one of four paired comparisons (Fig. 1*B*). When healing was compared with UW CECs, a two-fold change cutoff was used, resulting in more than 3,000 probe sets differentially expressed in NL and DM corneas. When DM CECs were compared with NL CECs, a 1.5-fold change cutoff was used because a much small number of differentially expressed genes was detected: 772 (397 increase and 377 decrease) in UW CECs and 1,888 probe sets (636 increase and 1,253 decrease) in healing CECs. Supplementary Table 1 lists the differentially expressed genes (probe sets). Table 1 lists the top 10 most up- or downregulated genes in four paired comparisons.

Pair 1: Healing Versus UW CECs in NL Corneas

The most elevated gene is S100A9 (705-fold), which is known to form a heterodimer with S100A8 (249-fold increase), both of which are highly inducible genes in epithelial cells (15). Its deficiency was associated with nonhealing venous leg ulcers (16). Prominent among greatly downregulated genes is CXCL14, a homeostatic chemokine that is expressed in basal epidermal keratinocytes (17,18). The expression patterns of S100A9 and CXCL14 were verified by real-time PCR (Fig. 2*A* and *B*).

Pair 2: Healing Versus UW CECs in DM Corneas

Compared with NL, 288 more probe sets were differentially expressed in the healing CECs of DM corneas, and 2,497 probe sets showed altered expression in both NL and DM CECs. Among the 10 most highly upregulated genes, 9 were also found in DM corneas with comparable fold changes. Tenascin C (Tnc) was replaced by podoplanin (Pdpn), a marker of lung injury (19), in DM CECs. On the downregulated gene list, Wnt2 was worthy of mention because it was not expressed in UW CECs. The downregulation of Wnt2 in DM compared with NL healing CECs was verified by real-time PCR (Fig. 2*C*).

Pair 3: DM Versus NL UW CECs

Compared with healing versus UW CECs in pairs 1 and 2, there were fewer differentially expressed genes in DM versus NL CECs, with much lower –fold changes. Thus, we lowered the cutoff value to 1.5-fold changes. The most highly up- and downregulated genes were Ephx2, known to contribute to renal injury during diabetes (20), and C1ql3, a gene only found in the central nerve system to regulate synapse formation (21), respectively. Upregulation of Ephx2 in DM CECs was verified by real time PCR (Fig. 2*D*)

Pair 4: DM Versus NL Healing CECs

Compared with homeostatic cells, a relatively large number of genes were differentially expressed: 1,888 probe sets in DM versus NL healing CECs. Among the

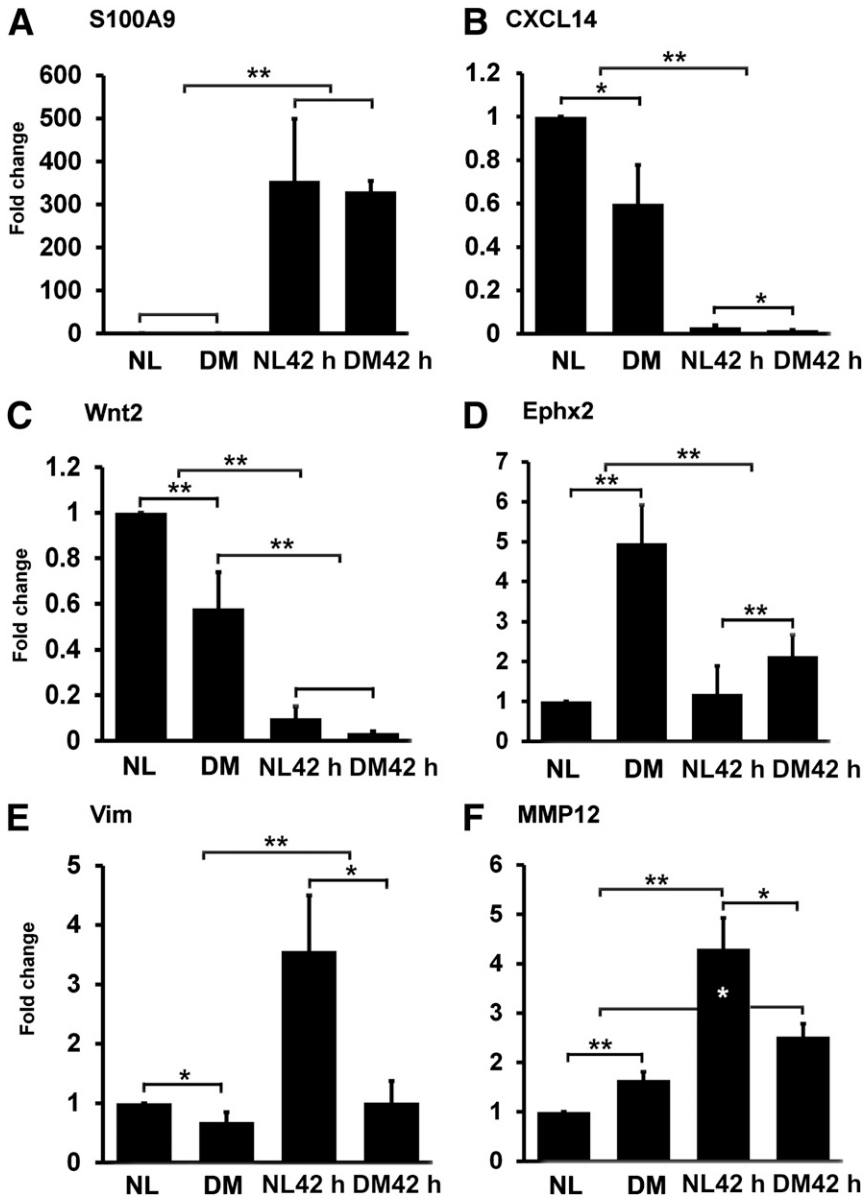

Figure 2—Real-time PCR verification of the expression patterns of six selected genes in healing vs. homeostatic CECs in NL rat corneas. The RNA samples were obtained as described in Fig. 1. The scraped CECs from NL and STZ-DM rat corneas for creating a wound were marked as 0 h and from the wound bed at 42 hpw and subjected to real-time PCR with primers specific for S100A9 (*A*), CXCL14 (*B*), Wnt2 (*C*), Ephx2 (*D*), Vim (*E*), and MMP12 (*F*). The data are presented as fold changes over non-DM, homeostatic CECs (1). Three samples were collected from three rats for each condition, and two independent experiments were performed. $^{*}P < 0.05$; $^{**}P < 0.01$.

105 highly induced probe sets, only 17 probe sets represent known genes, including Ephx2. On the other hand, many probe sets with downregulated expression in DM, compared with in NL healing CECs, contained gene identities. These include vimentin, ATF3, Wnt2, Tnc, peroxidasin (a gene associated with anterior segment dysgenesis (22) and MMP12. Figure 2*E* and *F* show the verifications of the expression patterns of vimentin and MMP12.

Among the 56 genes listed in Table 1, the expression patterns of 17 genes were confirmed in one or more DM models by real-time PCR and/or immunohistochemistry.

Decreased Expression of TGF-β3 in Healing CECs of Diabetic Corneas

Gene ontology (GO) analysis of 1,888 probe sets revealed many signaling pathways were altered, including pathways mediated by IL-1 (1.02e-3, 22/132, also see Fig. 3), HGF (2.8e-314/75), MMP (1.58e-4, 23/124), and TGFβ (7.39e-3, 43/360). Similar to GO Analysis, enrichment analysis of genes differentially expressed in DM versus NL healing CECs revealed TGFβ-dependent epithelial-mesenchymal transition to be a major event altered therein. Hence, we focused on TGFβ signaling pathways.

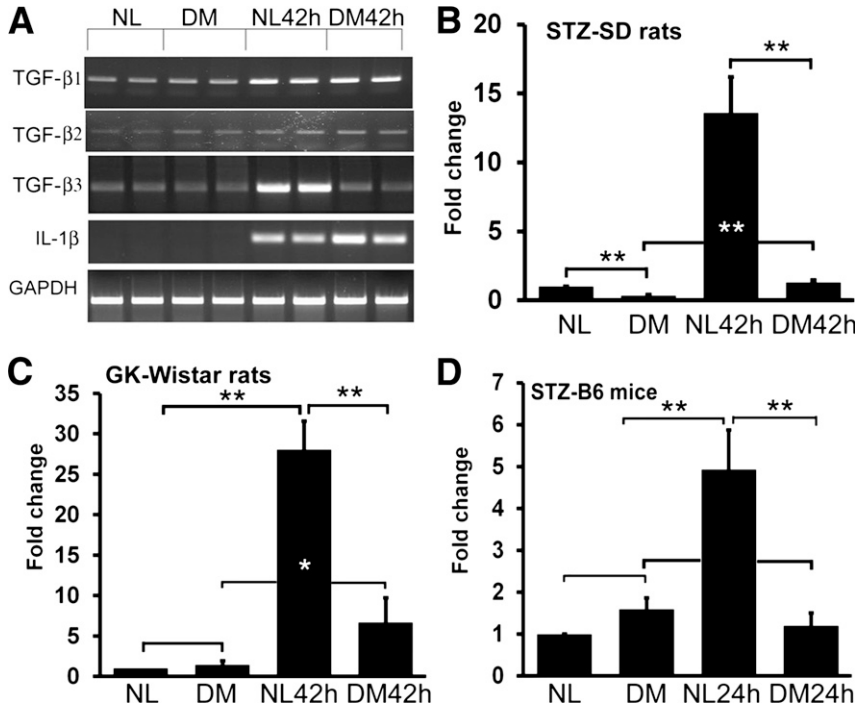

Figure 3—mRNA Expression of TGFβ isoforms detected by RT-PCR and verification of TGFβ3 expression by real-time PCR. The RNA samples were obtained as described in Fig. 1. The scraped CECs from NL and STZ-DM rat and mouse corneas for creating a wound were marked as UW and from the wound bed at 42 hpw (rats) or 24 hpw (mice) and were subjected to RT-PCR with GAPDH as the internal control and IL-1β as a positive control. The data were presented as fold changes over non-DM, homeostatic CECs (1). For each condition three samples were collected from three rats/mice. Four independent experiments were performed: two with SD and STZ-SD, one with Wistar and GK rats, and one with B6 and STZ-B6 mice.*$P < 0.05$; **$P < 0.01$.

To assess the expression patterns of the TGFβ family, real-time RT-PCR was performed (Fig. 3*A*) using STZ-SD rats. All three isoforms were detected, whereas mRNA for IL-1β (as a control) was undetectable in UW NL and DM CECs. Wounding induced Il-1β expression at the mRNA levels, and this upregulation was more apparent in DM healing CECs. The levels of TGFβ1 were also elevated in healing CECs; however, no difference was detected between DM and NL corneas (Fig. 3*B*). The levels of TGFβ2 were consistent under four conditions. TGFβ3 was greatly upregulated in the healing CECs of NL, but the levels of TGFβ3 in DM CECs remained at a level comparable to that of UW CECs. We have established three rodent diabetic models: STZ-SD rats (4,7), GK rats (6), and STZ-B6 mice. The expression of TGFβ3 was further assessed by real-time PCR, which showed significant upregulation in the healing CECs of NL, but not DM, corneas in all three rodent models (Fig. 3*B–D*).

The expression and distribution of TGF-β3 in were also assessed using immunohistochemistry (Fig. 4). Although TGF-β3 abundantly stained the entire healing corneal epithelial sheet, from the leading edge to the border region between the cornea and limbus in SD rat corneas, only a few TGF-β3 positive cells were found at the leading edge of the migratory epithelial sheet in type 1 DM rat corneas; the rest of the epithelial sheet stained low or negative.

TGF-β3 is Necessary for Proper Wound Healing

We next investigated whether TGF-β3 is required for wound healing in NL rats. We used subconjunctival injection of siRNA in Wistar rats and observed a significant delay in TGFβ–specific but not the control siRNAs compared with the control rats (Fig. 5*A*). Western blotting analysis of CECs revealed a basal expression of TGF-β3 in UW CECs and elevated levels in healing CECs in the Wistar rat, and this wounding-induced TGFβ3

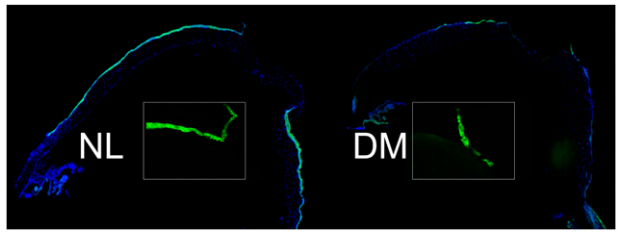

Figure 4—Immunohistochemistry of TGF-β3 distribution in healing and UW corneas. The corneas of SD and STZ-SD were wounded and O.C.T. snap frozen at 42 hpw, followed by sectioning and immunostaining with antibodies against TGF-β3; DAPI was used to stain nuclei. Low magnification (×5) images of the entire cornea were taken and images stitched to present the whole from limbus to wound center. Inserts are high magnification (×20) images of the leading edge. The figure is representative of three corneas per condition from two independent experiments.

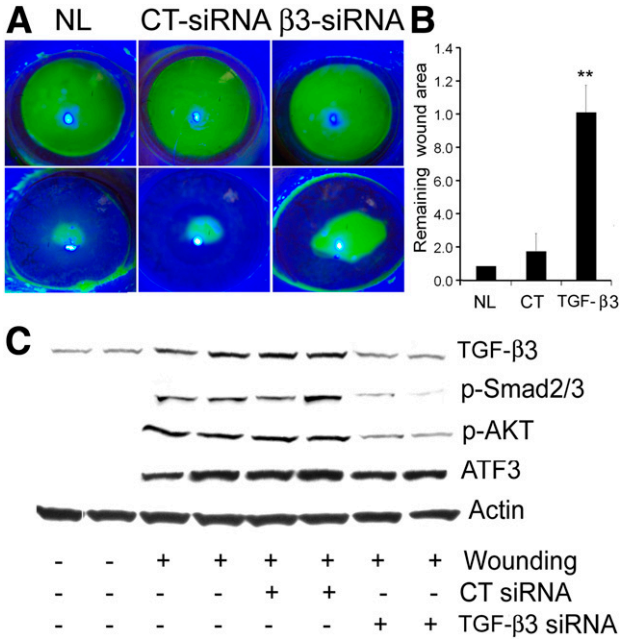

Figure 5—Effects of siRNA knockdown of TGF-β3 on corneal epithelial wound healing in Wistar rats. *A*: TGF-β3 specific and control, nonspecific siRNA were injected into subconjunctival space at two sites (10 μL of 10 μmol/L each site) of NL-SD rats 6 h before wounding. A 5-mm wound was made in the central cornea and allowed to heal for 42 h, fluorescence stained, and photographed. *B*: Changes in the mean of the remaining wound areas in pixels were calculated by Adobe Photoshop software ($n = 5$). $^{**}P < 0.01$. *C*: CECs collected during wounding (first two lanes) and 42 hpw were extracted and subjected to Western blotting with list antibodies. Two samples of five from each condition are shown with actin as the internal control. These figures are representatives of five corneas per condition from two independent experiments.

upregulation was knocked down by TGFβ3–specific siRNA. In UW CECs, there was no detectable phosphorylation of Smad2/3 and AKT, and in healing CECs, both signaling molecules were phosphorylated. Consistent with downregulated TGF-β3 levels, the phosphorylation of these proteins was also dampened, whereas the expression of ATF3, a stress responsive transcription factor with a similar expression pattern to TGF-β3 (Table 1), was not affected (Fig. 5*B*).

Exogenous TGF-β3 Accelerates Delayed Epithelial Wound Closure in DM Corneas

Whether exogenously added TGF-β3 in diabetic corneas accelerates delayed epithelial wound closure in GK and STZ-B6 mice was assessed next. In GK rat corneas, 40 ng TGF-β3 in 20 μL was injected 4 h before to epithelial debridement and substantially increased the rate of wound closure (Fig. 6*A* and *B*) and enhanced Smad2/3 phosphorylation in healing CECs (Fig. 6*C*). To assess if exogenously added TGF-β3 affects the isoform expression, antibodies against TGF-β1–β3 were used for Western blotting. Although TGF-β1 was upregulated in healing DM CECs, exogenously added TGF-β3 appeared to have no effects on its expression. The levels of TGF-β2 were low and unchanged in all the samples. Interestingly, exogenously applied TGF-β3 increased TGF-β3 expression. Although some elevated active TGF-β3 molecules could be from exogenously added TGF-β3 (15 kDa), the latent form (47 kDa) can only be from endogenous sources, indicating an autoregulation of TGF-β3 expression in rat corneas.

In STZ-B6 mice, the addition of TGF-β significantly increased the rate of epithelial closure at 16 and 24 hpw (Fig. 7*A* and *B*). When Serpine1, a common target of TGF-β (23), as an example, was used, our data showed that its mRNA levels were correlated to the levels of TGF-β3 activity and to that of the rates of wound closure in NL and DM mice (Fig. 7*C*).

TGF-β3 Expression in Cultured Human UW and PW Corneas

Delayed epithelial wound healing has also been shown in organ-cultured human corneas (2). We obtained NL and DM corneal cryostat sections without (direct embedded in O.C.T.) or with epithelial wounding, which were allowed to heal in an organ culture setting (2), and assessed TGF-β3 expression in these corneas using confocal microscopy (Fig. 8). In UW corneas, there were detectable levels of TGF-β3 in the epithelial layer. In the PW cornea with healed epithelial wound (2), all cell layers were positive with a strong TGF-β3 immunoreactivity in NL corneas, whereas weak staining was detected in DM CECs.

DISCUSSION

In this study, we used genome-wide cDNA microarrays to compare the gene expression profiles of healing versus UW and DM versus NL CECs. Our results revealed that wounding dramatically altered the expression of a large number of genes in NL and DM corneas. Bioinformatics revealed many TGFβ-mediated signaling pathways, and biological processes were altered. Using three diabetic mouse and rat models, we showed that TGF-β3 activity is required for proper wound healing in NL corneas, whereas exogenously added TGF-β3 promotes epithelial wound healing in the corneas of type 1 DM rats and mice and type 2 DM rats. The effects of TGF-βs on epithelial wound closure are related to its ability to activate Smad-dependent and -independent pathways, to modulate its own expression, and to mediate target gene expression. Taken together, our study suggests that the hyperglycemia-suppressed genes, such as TGFβ3 and Serpine1, might be used as therapeutic reagents to accelerate delayed epithelial wound healing in diabetic corneas.

The genome-wide cDNA array analyses revealed a greatly altered expression of genes in response to wounding and illustrated genes affected by hyperglycemia at a much larger scale in CECs. Unlike previous

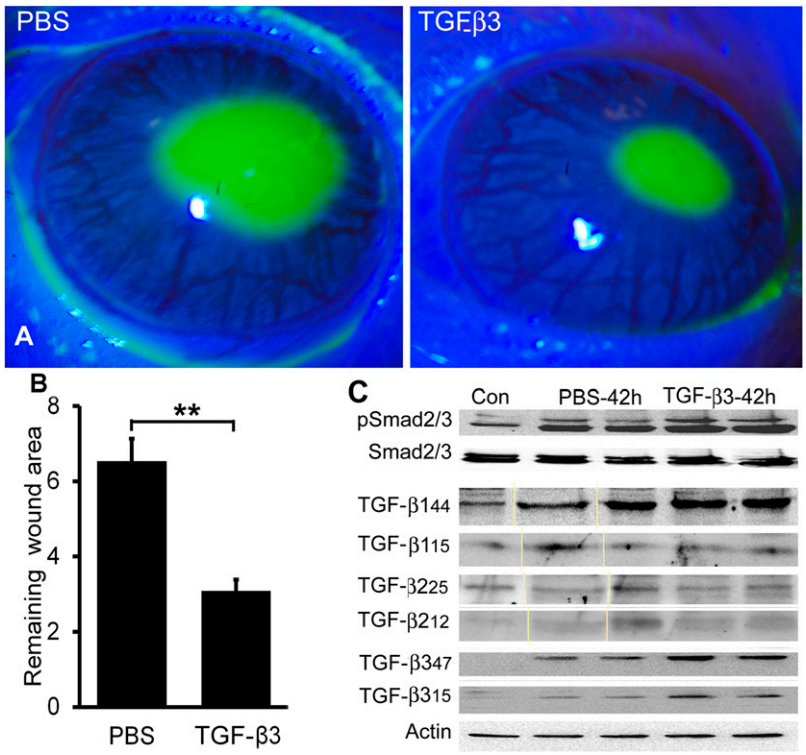

Figure 6—Effects of TGF-β3 on epithelial wound closure in GK rat corneas. *A*: Recombinant TGF-β3 (40 ng), with PBS as the control, was injected into subconjunctival space at two sites (10 μL each) of GK rats 4 h before wounding. A corneal epithelial wound (5-mm diameter) was made and allowed to heal for 42 h and then fluorescence stained and photographed. *B*: Changes in the mean of the remaining wound areas in pixels were calculated by Adobe Photoshop software (n = 5) with P value listed. *C*: CECs collected during wounding (Con) and 42 hpw in PBS- and TGF-β3–treated corneas were extracted and subjected to Western blotting with list antibodies. Two of five samples from PW corneas are shown with actin as the internal control. The anti-TGF-β1–3 antibodies recognize latent (44, 25, and 47 kDa, respectively) and active (15, 12, and 15 kDa, respectively) forms, giving two bands in Western blotting. These figures are representatives of five corneas per condition from two independent experiments. $^{**}P < 0.01$.

studies using limited arrays and RNA isolated from the cornea (24,25), our approach used CECs and thus avoided false-positive results from infiltration of immune cells in the stroma. Although most of the genes detected with differential expression are likely from epithelial cells, a small portion of differentially expressed genes might be from dendritic cells because they migrate with the healing epithelial sheets (26). Moreover, 8 weeks of hyperglycemia represented an early stage of DM when a significant delay of epithelial wound closure has begun (4,7). This allows us to characterize early events of diabetes complication, which can be effectively intervened with or even reversed. With these advantages, our genome-wide cDNA array revealed a large number of genes (probe sets) differentially expressed, and the expression of many genes was verified by other means and/or consistent with their known function, further validating the value of the genome-wide microarray data.

Comparison of healing DM with healing NL CECs revealed that 1,888 probe sets had altered expression. Intriguingly, of the 36 probe sets with more than threefold increases in DM healing versus NL healing, only 4 are identified genes; the rest were derived from DNA sequence tags without gene identities. Among four genes, the upregulation of Ephx2, which was linked to subclinical cardiovascular disease in the Diabetes Heart Study (27), is most interesting because it was shown to increase manifestations of diabetic nephropathy in mice (20). There were 17 genes with fourfold decreases, and among them, ATF3 and CEACAM1 have been shown to be associated with DM (28,29). The role of Ephx2, ATF3, and Ceacam1 or the lack thereof in diabetic corneas remains to be determined.

GO analyses revealed that the signaling pathway mediated by TGFβ-Smad was impaired in DM healing CECs. Because TGF-β has been known to play a key role in corneal wound healing and fibrosis and the major cellular source of TGF-β in corneal wounds is the epithelium (30), we assessed the expression of three TGFβ isoforms and observed that hyperglycemia had no effects on TGFβ1 but greatly suppressed TGFβ3 in DM healing CECs. Earlier studies reported that TGF-β1 and β2 are both seen within the corneal epithelium in the cornea and the stroma in the injured cornea, whereas TGF-β3 is not found in the anterior eye (for review see (31)). More recent studies reported that TGF-β3 was found in the

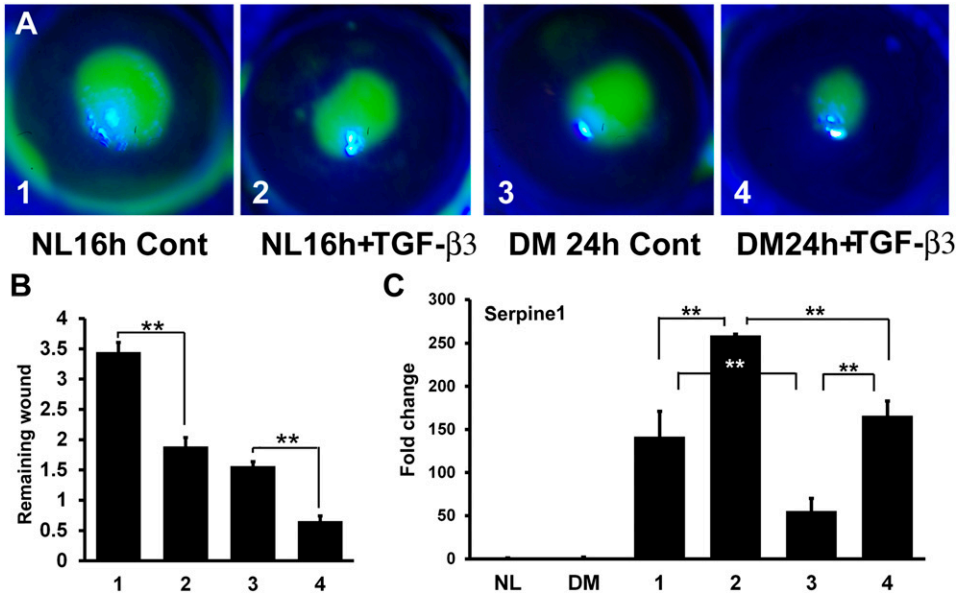

Figure 7—Effects of TGF-β3 on epithelial wound closure in B6 and STZ-B6 mouse corneas. *A*: Recombinant TGF-β3 (14 ng), with PBS as the control, was injected into subconjunctival space at inferior side of B6 and STZ-B6 mice 4 h before wounding. A 2-mm epithelial wound was made and allowed to heal for 16 h in B6 mice and for 24 h in STZ-B6 mice, and then fluorescence stained, and photographed. NL cornea injected with PBS (*1*), NL cornea injected with TGF-β3 (*2*), DM (STZ) cornea injected with PBS (*3*), and DM cornea injected with TGF-β3 (*4*). *B*: Changes in the mean of the remaining wound areas in pixels were calculated by Adobe Photoshop software ($n = 5$) with *P* value. *C*: CECs collected during wounding (first two lanes) and at 16 hpw (1 and 2) or 24 hpw (3 and 4) in PBS (1 and 3) and TGF-b3 (2 and 4) treated corneas were extracted and subjected to real-time PCR analysis for Serpine1 expression ($n = 3$). $^{**}P < 0.01$.

basal cells of regenerating areas as well as in uninjured regions of the cornea after corneal injury (32). We presented strong evidence of upregulation of TGF-β3 expression in three animal models as well as in cultured human corneas. Hence, we conclude that TGF-β3 is expressed in CECs and its expression is upregulated in response to wounding in NL corneas. More strikingly, we showed almost total suppression of wound-induced TGF-β3 upregulation in diabetic corneas, suggesting a unique role of TGF-β3 in mediating epithelial wound closure. To our knowledge, our study is the first to unambiguously demonstrate the suppressive effects of hyperglycemia on the expression of TGFβ3 but not TGFβ1 at mRNA and protein levels in response to wounding.

Although TGFβ1, β2, and β3 share 60–80% identity, they are encoded by distinct genes, have different sequences in promoters, and exhibit different physiological and pathological activities in vivo (33). The importance of TGF-β in maintaining tissue homeostasis and in regulating wound healing in the cornea has been

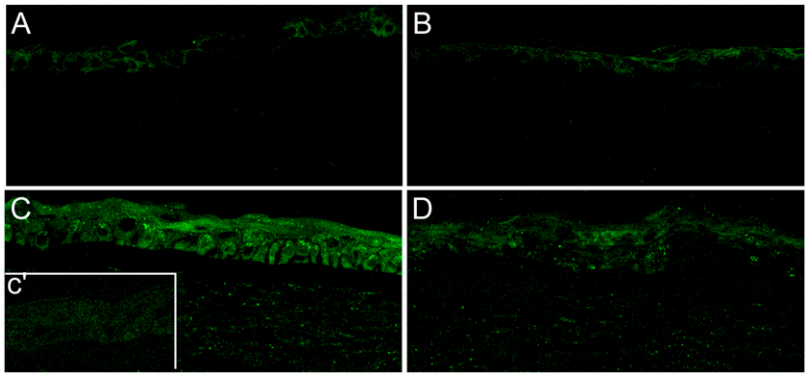

Figure 8—Expression and distribution of TGF-β3 in cultured human NL and DM corneas with or without wounding. Human diabetic corneas (*B* and *D*) and age-matched controls (*A* and *C*) were directly processed for (*A* and *B*) or were wounded (6 mm) before organ culture, as described by Saghizadeh et al. (50). At 10 days after wounding, corneas were frozen in O.C.T. *C*: The cryostat sections were stained with rabbit anti-human TGF-β3 antibody with nonspecific rabbit IgG as the negative control (insert c' in NL healed cornea). Photos show merged images of confocal microscopy and are the representative of two animals in each group.

reported (for review see [31]). The response of TGF-β to wounding can be mediated through Smad-dependent and -independent signaling pathways in a manner dependent on cell type and context (34–37). Among Smad-independent pathways, the PI3K/AKT pathway plays a significant role in regulating TGF-β–mediated responses (35). Demonstration that wound-induced TGF-β3 expression in CECs is sensitive to hyperglycemia suggests a distinctive regulation and a unique role of the isoform in modulating epithelial wound healing.

To define the role of identified genes, we administrated siRNA or recombinant TGFβ3 to the corneas using subconjunctival injection, which is a common procedure performed at ophthalmologists' office to deliver drugs to treat corneal diseases and glaucoma and has been shown to allow bevacizumab to penetrate the intact cornea (38–40). Using subconjunctival injection to deliver TGF-β3 siRNA in NL corneas and recombinant TGF-β3 in NL and DM corneas, we demonstrated that TGF-β3 upregulation in response to epithelial wounding contributes to epithelial wound healing and activates canonical and noncanonical signaling pathways. The altered expression of TGF-β3 was also confirmed in cultured human corneas after wound healing, indicating the relevance of the study. Moreover, we demonstrated that exogenous TGF-β3 partially restored the healing rate of epithelial wounds in diabetic corneas of three rodent models, suggesting an important role for the isoform in mediating epithelial response to injury. Strikingly, we discovered that exogenously applied TGF-β3 elevated the levels of latent TGF-β3 but not TGF-β1 or β2 at the protein levels, suggesting an autoregulated expression of TGF-β3 in the healing CECs such as that observed in the mouse skin carcinogenesis model (41). Although the mechanisms underlying hyperglycemia-suppressed wound-induced TGF-β3 expression are unclear, early inhibitory effects of hyperglycemia on TGF-β3 expression, which differs from that of TGF-β1 (42), may exacerbate the suppression of TGF-β3 upregulation in response to wounding. Finally, we showed that the expression of Serpine1, a well-known TGFβ target gene (43,44), is correlated to the activity of TGF-β3 in healing CECs of NL and DM corneas.

The discovery that TGF-β has a unique role in mediating corneal epithelial wound healing is of great significance because *1*) the major cellular source of TGF-β in corneal wounds is the epithelium (30); *2*) TGF-β3, in contrast to TGF-β1, is considered an antifibrotic (45); *3*) TGF-β3 halts fibroblast migration and selectively promotes reepithelialization in the skin wounds (46), indicating a critical role in skin wound healing; and *4*) recombinant TGF-β3 has been undergoing phase 3 clinical trials as an antiscarring agent for adult skin wounds (45,47,48). The trial was considered a failure due to increased angiogenesis in postsurgery skin (45). However, unlike the pathogenesis of diabetic retinopathy, nephropathy, and atherosclerotic plaque where there is excessive angiogenesis, blood vessel growth is impaired in diabetic wound healing (49). Hence, TGF-β3 may potentially be used as a useful therapy to treat delayed wound healing in the cornea and in the skin for the benefit of accelerating wound healing and reducing inflammation that should outweigh adverse effects caused by neovascularization, which may not occur during diabetic wound healing (49). Further study of the mechanism of the action and target gene expression of TGF-β3 in the corneal and skin may lead to clinical trials of TGF-β3 for its unique function in epithelial cells under hyperglycemia conditions.

Acknowledgments. The authors thank Drs. Ashok Kumar, Jia Yin, and Patrick Lee of Wayne State University School of Medicine for critical reading of the manuscript and are grateful to Dr. Alexander V. Ljubimov, Regenerative Medicine Institute, Cedars-Sinai Medical Center, for providing human corneal cryostat sections.

Funding. The authors received support from National Institutes of Health/National Eye Institute R01-EY-10869, R01-EY-17960 (to F.-S.X.Y.), P30-EY-04078 (National Eye Institute core to Wayne State University), and Research to Prevent Blindness (to Kresge Eye Institute).

Duality of Interest. No potential conflicts of interest relevant to this article were reported.

Author Contributions. I.B., H.S., and N.G. performed laboratory testing, and edited and checked the accuracy of the manuscript. F.W. performed RNA preparation for microarray and part of the immunohistochemistry analysis. X.M. performed laboratory testing and data analysis. W.C. performed bioinformatics analysis of cDNA array. Z.L. contributed to discussion and reviewed the manuscript. F.-S.X.Y. was responsible for study design and recruitment, contributed to sample collection and data analysis, and reviewed and edited the manuscript. F.-S.X.Y. is the guarantor of this work and, as such, had full access to all of the data in the study and takes responsibility for the integrity of the data and the accuracy of the data analysis.

References

1. Kaji Y. Prevention of diabetic keratopathy. Br J Ophthalmol 2005;89:254–255
2. Kabosova A, Kramerov AA, Aoki AM, Murphy G, Zieske JD, Ljubimov AV. Human diabetic corneas preserve wound healing, basement membrane, integrin and MMP-10 differences from normal corneas in organ culture. Exp Eye Res 2003;77:211–217
3. Zagon IS, Sassani JW, McLaughlin PJ. Insulin treatment ameliorates impaired corneal reepithelialization in diabetic rats. Diabetes 2006;55:1141–1147
4. Xu K, Yu FS. Impaired epithelial wound healing and EGFR signaling pathways in the corneas of diabetic rats. Invest Ophthalmol Vis Sci 2011;52:3301–3308
5. Inoue A, Watanabe T, Tominaga K, et al. Association of hnRNP S1 proteins with vimentin intermediate filaments in migrating cells. J Cell Sci 2005;118:2303–2311
6. Wang F, Gao N, Yin J, Yu FS. Reduced innervation and delayed re-innervation after epithelial wounding in type 2 diabetic Goto-Kakizaki rats. Am J Pathol 2012;181:2058–2066
7. Yin J, Huang J, Chen C, Gao N, Wang F, Yu FS. Corneal complications in streptozocin-induced type I diabetic rats. Invest Ophthalmol Vis Sci 2011;52:6589–6596

8. Schultz RO, Van Horn DL, Peters MA, Klewin KM, Schutten WH. Diabetic keratopathy. Trans Am Ophthalmol Soc 1981;79:180–199
9. Pflugfelder SC. Is autologous serum a tonic for the ailing corneal epithelium? Am J Ophthalmol 2006;142:316–317
10. Chi C, Trinkaus-Randall V. New insights in wound response and repair of epithelium. J Cell Physiol 2013;228:925–929
11. Martin P. Wound healing—aiming for perfect skin regeneration. Science 1997;276:75–81
12. Bikbova G, Oshitari T, Tawada A, Yamamoto S. Corneal changes in diabetes mellitus. Curr Diabetes Rev 2012;8:294–302
13. Xu KP, Li Y, Ljubimov AV, Yu FS. High glucose suppresses epidermal growth factor receptor/phosphatidylinositol 3-kinase/Akt signaling pathway and attenuates corneal epithelial wound healing. Diabetes 2009;58: 1077–1085
14. Wang F, Song YL, Li DH, et al. Type 2 diabetes mellitus impairs bone healing of dental implants in GK rats. Diabetes Res Clin Pract 2010;88: e7–e9
15. Gao N, Sang Yoon G, Liu X, et al. Genome-wide transcriptional analysis of differentially expressed genes in flagellin-pretreated mouse corneal epithelial cells in response to Pseudomonas aeruginosa: involvement of S100A8/A9. Mucosal Immunol 2013;6:993–1005
16. Trøstrup H, Lundquist R, Christensen LH, et al. S100A8/A9 deficiency in nonhealing venous leg ulcers uncovered by multiplexed antibody microarray profiling. Br J Dermatol 2011;165:292–301
17. Schaerli P, Willimann K, Ebert LM, Walz A, Moser B. Cutaneous CXCL14 targets blood precursors to epidermal niches for Langerhans cell differentiation. Immunity 2005;23:331–342
18. Meuter S, Moser B. Constitutive expression of CXCL14 in healthy human and murine epithelial tissues. Cytokine 2008;44:248–255
19. Navarro A, Perez RE, Rezaiekhaligh MH, Mabry SM, Ekekezie II. Polarized migration of lymphatic endothelial cells is critically dependent on podoplanin regulation of Cdc42. Am J Physiol Lung Cell Mol Physiol 2011; 300:L32–L42
20. Elmarakby AA, Faulkner J, Al-Shabrawey M, Wang MH, Maddipati KR, Imig JD. Deletion of soluble epoxide hydrolase gene improves renal endothelial function and reduces renal inflammation and injury in streptozotocin-induced type 1 diabetes. Am J Physiol Regul Integr Comp Physiol 2011; 301:R1307–R1317
21. Bolliger MF, Martinelli DC, Südhof TC. The cell-adhesion G protein-coupled receptor BAI3 is a high-affinity receptor for C1q-like proteins. Proc Natl Acad Sci U S A 2011;108:2534–2539
22. Khan K, Rudkin A, Parry DA, et al. Homozygous mutations in PXDN cause congenital cataract, corneal opacity, and developmental glaucoma. Am J Hum Genet 2011;89:464–473
23. Kang Y, Chen CR, Massagué J. A self-enabling TGFbeta response coupled to stress signaling: Smad engages stress response factor ATF3 for Id1 repression in epithelial cells. Mol Cell 2003;11:915–926
24. Cao Z, Wu HK, Bruce A, Wollenberg K, Panjwani N. Detection of differentially expressed genes in healing mouse corneas, using cDNA microarrays. Invest Ophthalmol Vis Sci 2002;43:2897–2904
25. Varela JC, Goldstein MH, Baker HV, Schultz GS. Microarray analysis of gene expression patterns during healing of rat corneas after excimer laser photorefractive keratectomy. Invest Ophthalmol Vis Sci 2002;43:1772–1782
26. Gao N, Yin J, Yoon GS, Mi QS, Yu FS. Dendritic cell-epithelium interplay is a determinant factor for corneal epithelial wound repair. Am J Pathol 2011; 179:2243–2253
27. Burdon KP, Lehtinen AB, Langefeld CD, et al. Genetic analysis of the soluble epoxide hydrolase gene, EPHX2, in subclinical cardiovascular disease in the Diabetes Heart Study. Diab Vasc Dis Res 2008;5:128–134
28. Kim JY, Lee SH, Song EH, et al. A critical role of STAT1 in streptozotocin-induced diabetic liver injury in mice: controlled by ATF3. Cell Signal 2009; 21:1758–1767
29. Najjar SM. Regulation of insulin action by CEACAM1. Trends Endocrinol Metab 2002;13:240–245
30. Stramer BM, Austin JS, Roberts AB, Fini ME. Selective reduction of fibrotic markers in repairing corneas of mice deficient in Smad3. J Cell Physiol 2005;203:226–232
31. Tandon A, Tovey JC, Sharma A, Gupta R, Mohan RR. Role of transforming growth factor Beta in corneal function, biology and pathology. Curr Mol Med 2010;10:565–578
32. Huh MI, Chang Y, Jung JC. Temporal and spatial distribution of TGF-beta isoforms and signaling intermediates in corneal regenerative wound repair. Histol Histopathol 2009;24:1405–1416
33. Saika S. TGFbeta pathobiology in the eye. Lab Invest 2006;86:106–115
34. Goc A, Choudhary M, Byzova TV, Somanath PR. TGFβ- and bleomycin-induced extracellular matrix synthesis is mediated through Akt and mammalian target of rapamycin (mTOR). J Cell Physiol 2011;226:3004–3013
35. Hong M, Wilkes MC, Penheiter SG, Gupta SK, Edens M, Leof EB. Non-Smad transforming growth factor-β signaling regulated by focal adhesion kinase binding the p85 subunit of phosphatidylinositol 3-kinase. J Biol Chem 2011;286:17841–17850
36. Lu L, Wang J, Zhang F, et al. Role of SMAD and non-SMAD signals in the development of Th17 and regulatory T cells. J Immunol 2010;184:4295–4306
37. Holm TM, Habashi JP, Doyle JJ, et al. Noncanonical TGFβ signaling contributes to aortic aneurysm progression in Marfan syndrome mice. Science 2011;332:358–361
38. Chong RS, Su DH, Tsai A, et al. Patient acceptance and attitude toward an alternative method of subconjunctival injection for the medical treatment of glaucoma. J Glaucoma 2013;22:190–194
39. Erdurmus M, Totan Y. Subconjunctival bevacizumab for corneal neovascularization. Graefes Arch Klin Exp Ophthalmol 2007;245:1577–1579
40. Dastjerdi MH, Sadrai Z, Saban DR, Zhang Q, Dana R. Corneal penetration of topical and subconjunctival bevacizumab. Invest Ophthalmol Vis Sci 2011; 52:8718–8723
41. Rundhaug JE, Park J, Fischer SM. Uncoordinated regulation of mRNA expression of the three isoforms of transforming growth factor-beta in the mouse skin carcinogenesis model. Mol Carcinog 1997;18:115–126
42. Liu G, Ding W, Neiman J, Mulder KM. Requirement of Smad3 and CREB-1 in mediating transforming growth factor-beta (TGF beta) induction of TGF beta 3 secretion. J Biol Chem 2006;281:29479–29490
43. Samarakoon R, Overstreet JM, Higgins SP, Higgins PJ. TGF-β1 → SMAD/p53/USF2 → PAI-1 transcriptional axis in ureteral obstruction-induced renal fibrosis. Cell Tissue Res 2012;347:117–128
44. Samarakoon R, Higgins PJ. Integration of non-SMAD and SMAD signaling in TGF-beta1-induced plasminogen activator inhibitor type-1 gene expression in vascular smooth muscle cells. Thromb Haemost 2008;100: 976–983
45. Henderson J, Ferguson MW, Terenghi G. The reinnervation pattern of wounds and scars after treatment with transforming growth

factor β isoforms. J Plast Reconstr Aesthet Surg 2012;65: e80–e86

46. Han A, Bandyopadhyay B, Jayaprakash P, et al. The anti-motility signaling mechanism of TGFβ3 that controls cell traffic during skin wound healing. Biol Open 2012;1:1169–1177
47. Laverty HG, Occleston NL, Johnson M, et al. Effects of avotermin (transforming growth factor β3) in a clinically relevant pig model of long, full-thickness incisional wounds. J Cutan Med Surg 2010;14:223–232
48. Bush J, So K, Mason T, Occleston NL, O'Kane S, Ferguson MW: Therapies with emerging evidence of efficacy: avotermin for the improvement of scarring. Dermatol Res Pract 2010;2010;Article ID 690613
49. Costa PZ, Soares R. Neovascularization in diabetes and its complications. Unraveling the angiogenic paradox. Life Sci 2013;92:1037–1045
50. Saghizadeh M, Kramerov AA, Tajbakhsh J, et al. Proteinase and growth factor alterations revealed by gene microarray analysis of human diabetic corneas. Invest Ophthalmol Vis Sci 2005;46:3604–3615